SIMULATING ATMOSPHERIC FLOWS IN THE VICINITY OF A WATER BASIN*

M. S. Yudin
Institute of Computational Mathematics and Mathematical Geophysics, Novosibirsk, Russia
e-mail: yudin@ommfao.sscc.ru

K. Wilderotter
Fachbereich Allgemeinwissenschaften, Fachhochschule Rosenheim, Germany
e-mail: wilderotter@fh-rosenheim.de

Эта работа является продолжением предыдущего исследования авторов по атмосферной циркуляции и переносу загрязнений в окрестности водного бассейна вблизи города. Проведено моделирование переноса примеси над пологим холмом с помощью трехмерной модели, основанной на конечных элементах, при этом данные по температуре и ветру получены с помощью трехмерной конечно-разностной метеорологической модели. Общий характер переноса примеси, рассчитанный по модели, находится в качественном соответствии с теоретическими представлениями. Проведено сравнение между результатами, полученными негидростатической и гидростатической конечно-разностными моделями при моделировании метеорологического потока над пологим холмом в окрестности водного бассейна. При сравнении с данными наблюдений результаты гидростатической модели содержат большие отклонения, при этом негидростатическая модель моделирует поля температуры и ветра с хорошей точностью.

Introduction

The mesoscale meteorological phenomena that take place at coastal sites received much attention of researchers in recent years. This is due to the fact that these phenomena may have a considerable impact on local climate.

The problem of simulating local climatic characteristics of aerosol transfer in the atmosphere in the vicinity of a water basin is also important from a computational viewpoint. It is vital to use efficient numerical algorithms in the domains of abrupt variation of calculated fields without using mesh refinement and suppressing spurious oscillations near the front of aerosol cloud propagation. In this paper a simple finite-element scheme is used, which is based on

*This research is part of work supported by the Department of Mathematical Sciences, RAS (Program N 3) and RFBR (Grant N 04-05-64562).

the so-called Petrov — Galerkin approach, which implies adding artificial viscosity in the flow direction. This scheme is highly accurate and robust.

Hydrostatic models have played a great role in the simulation of atmospheric flows that occur at land-water boundaries [1]. Later, the advent of nonhydrostatic models enabled a wider class of flow phenomena to be simulated, specifically small-scale phenomena as, for instance, sea breeze front propagation.

This paper originated from an attempt to realistically simulate the meteorological flows that occur at water-land boundaries. Here, even with low topography, the changes in roughness from water to land and local terrain variations produce dynamic effects that are difficult for simulating by hydrostatic models.

Special methods have been developed to correct the hydrostatic approach by parameterizing nonhydrostatic terrain effects in hydrostatic models [2, 3].

In this paper, a comparison is made between results produced by hydrostatic and nonhydrostatic versions of a small-scale meteorological model. The results obtained are further compared with observations carried out at a mast located at a low hill in a coastal zone.

The paper is organized as follows: the model equations and discretizations are described in Section 1. Section 2 is devoted to the substance transport in the atmosphere at high Reynolds numbers. The calculation algorithm here is based on the Petrov — Galerkin approach. In Section 3, results of model simulations of coastal site flows are shown both for hydrostatic and nonhydrostatic versions of the model. Conclusions to the paper are given in Section 4.

1. Model equations

The necessary input data for pollutant transport calculations are obtained from a small-scale meteorological model. The basic equations for motion, heat, moisture and continuity of the nonhydrostatic version of the model in a terrain-following coordinate system are as follows:

$$\frac{dU}{dt} + \frac{\partial P}{\partial x} + \frac{\partial (G^{13}P)}{\partial \eta} = f_1 (V - V_g) - f_2 W + R_u,$$

$$\frac{dV}{dt} + \frac{\partial P}{\partial y} + \frac{\partial (G^{23}P)}{\partial \eta} = -f_1 (U - U_g) + R_v,$$

$$\frac{dW}{dt} + \frac{1}{G^{1/2}} \frac{\partial P}{\partial \eta} + \frac{gP}{C_s^2} = f_2 U + g \frac{G^{1/2} \bar{\rho} \theta'}{\bar{\theta}} + R_w,$$

$$\frac{d\theta}{dt} = R_\theta, \quad \frac{ds}{dt} = R_s,$$

$$\frac{1}{C_s^2} \frac{\partial P}{\partial t} + \frac{\partial U}{\partial x} + \frac{\partial V}{\partial y} + \frac{\partial}{\partial \eta} \left(G^{13} U + G^{23} V + \frac{1}{G^{1/2}} W \right) = \frac{\partial}{\partial t} \left(\frac{G^{1/2} \bar{\rho} \theta'}{\bar{\theta}} \right),$$

$$U = \bar{\rho} G^{1/2} u, \quad V = \bar{\rho} G^{1/2} v, \quad W = \bar{\rho} G^{1/2} w, \quad P = G^{1/2} p',$$

where p', θ' are deviations from the basic state pressure $\bar{p}$ and potential temperature $\bar{\theta}$, s is the specific humidity, C_s is the sound wave speed, u_g, v_g are components of the geostrophic wind representing the synoptic part of the pressure, η is the terrain-following coordinate transformation:

$$\eta = \frac{H (z - z_s)}{(H - z_s)},$$

z_s is the surface height, H is the height of the top of the model domain. Here $H = \text{const}$.

$$G^{1/2} = 1 - z_s/H, \quad G^{13} = \frac{1}{G^{1/2}}\left(\frac{\eta}{H} - 1\right)\frac{\partial z_s}{\partial x}, \quad G^{23} = \frac{1}{G^{1/2}}\left(\frac{\eta}{H} - 1\right)\frac{\partial z_s}{\partial y}.$$

For an arbitrary function φ

$$\frac{d\varphi}{dt} = \frac{\partial}{\partial t} + \frac{\partial u\varphi}{\partial x} + \frac{\partial v\varphi}{\partial y} + \frac{\partial \omega\varphi}{\partial \eta},$$

where

$$\omega = \frac{1}{G^{1/2}}W + G^{13}u + G^{23}v.$$

The terms R_u, R_v, R_ω, R_θ, R_s refer to subgrid-scale processes. As a turbulence parameterization, we use a simple scheme:

$$K_m = \begin{cases} l^2\sqrt{\frac{1}{2}}\left(\underline{D}^2\right)(1 - R_i), & R_i < 1, \\ 0, & R_i \geq 1, \end{cases}$$

$$R_i = \frac{g(d\ln\Theta dz)}{\underline{D}^2/2},$$

$$\underline{D} = \nabla\underline{u} + \underline{u}\nabla.$$

In the hydrostatic version of the model, the vertical velocity is not determined from the third equation of motion, as is the case in the nonhydrostatic version, but calculated diagnostically with the help of the continuity equation. At the top of the model domain in the hydrostatic version, we have a free surface that satisfies an additional evolutionary equation.

We approximate the advective terms in the model described above by the following difference operators:

$$\delta_d\varphi = \left[\varphi\left(d + \Delta d/2\right) - \varphi\left(d - \Delta d/2\right)\right]/\Delta d,$$

$$\varphi^d = \left[\varphi\left(d + \Delta d/2\right) + \varphi\left(d - \Delta d/2\right)\right]/2,$$

$$ADVX = \delta_x\left(u^x\left(\rho^x u^x\right)\right) + \delta_y\left(v^x\left(\rho^x u\right)^y\right) + \delta_z\left(\omega^x\left(\rho^x u\right)^z\right),$$

$$ADVY = \delta_x\left(u^y\left(\rho^y v\right)^x\right) + \delta_y\left(v^y\left(\rho^y v\right)^y\right) + \delta_z\left(\omega^y\left(\rho^y v\right)^z\right),$$

$$ADVZ = \delta_x\left(u^z\left(\rho^z w\right)^x\right) + \delta_y\left(v^x\left(\rho^z w\right)^y\right) + \delta_z\left(\omega^z\left(\rho^z w\right)^z\right),$$

$$ADVT = \delta_x\left(u\left(\rho\Theta\right)^x\right) + \delta_y\left(v\left(\rho\Theta\right)^y\right) + \delta_z\left(\omega\left(\rho\Theta\right)^z\right).$$

A more detailed description of the model and the numerical algorithms used in calculations can be found in [4].

2. Modeling of aerosol propagation

The convection-diffusion equation for the transport of substance in the atmosphere has the following form [6]:

$$\frac{\partial\Phi}{\partial t} = \nabla\cdot\left(\mathbf{K}\nabla\Phi - \mathbf{v}\Phi\right) - \lambda\Phi + f.$$

Here $\Phi(\mathbf{x}, t)$ is the aerosol concentration, $\mathbf{K}(\mathbf{x}, t)$ is the dispersion tensor, $\mathbf{v}(\mathbf{x}, t)$ is the wind velocity, $\lambda(\mathbf{x}, t)$ describes the chemical reactions, $f(\mathbf{x}, t)$ is the source or sink term, and $\mathbf{x} \in \mathbf{R}^d, d = 1, 2, 3$.

We discretize this problem by the so-called standard Galerkin method, sometimes also called the Bubnov — Galerkin method (see, e. g., [7]). This method gives good numerical results for moderate Reynolds numbers. However, for large Reynolds numbers, i. e. in case when advection strongly dominates diffusion, the results obtained by the standard Galerkin method are highly oscillatory and differ greatly from the exact solution. One way of suppressing the undesirable oscillations is the Petrov — Galerkin approach. For ease of the notation, let us describe this method in the following simplified statement. We assume that the process of aerosol transport is stationary and that there are no chemical reactions. Besides, we assume that $K = \text{const}$, $K \leq\leq 1$, and the velocity vector $\mathbf{v}$ is constant and normalized, that is, $|\mathbf{v}| = 1$. It should be noted, however, that the analysis can be easily generalized to other cases. We denote as $\nabla_v \Phi = v_x \dfrac{\partial \Phi}{\partial x} + v_y \dfrac{\partial \Phi}{\partial y} + v_z \dfrac{\partial \Phi}{\partial z}$ the derivative in the direction $\mathbf{v}$. Let the domain boundary Γ consist of parts Γ_1, Γ_2, Γ_3, and Γ_4.

Then our problem takes the following form:

$$-K\Delta\Phi + \nabla v\Phi = f,$$
$$\Phi = \Phi^D \quad \text{on} \quad \Gamma_2,$$
$$\frac{\partial \Phi}{\partial n} = 0 \quad \text{on} \quad \Gamma_1, \Gamma_3, \Gamma_4.$$

We use the standard notation for scalar product

$$(\Phi, \Psi) = \int\limits_{\Omega} \Phi\Psi d\Omega, (\nabla\Phi, \nabla\Phi) = \int\limits_{\Omega} \nabla\Phi \ \ \nabla\Psi d\Omega.$$

Multiplying this equation by the test function $\Psi + \delta\nabla_v\Psi$, where $\Psi = 0$ – Γ_2, and integrating over Ω, we obtain

$$K(\nabla\Phi, \nabla\Psi) - K\delta\left(\Delta\Phi, \nabla_v\Psi\right) + \left(\nabla_v\Phi, \Psi + \delta\nabla_v\Psi\right) = \left(f, \Psi + \delta\nabla\Psi_v\right),$$

where the term $K(\Delta\Phi, \Psi)$ was integrated by parts, δ is a positive parameter to be determined below. To formulate a discrete analog of this equation, we replace, by analogy with the standard Galerkin method, Φ and Ψ by piecewise linear approximations $\bar{\Phi}$ and $\bar{\Psi}$, which interpolate exactly at the triangulation nodes.

Since $\bar{\Phi}$ is piecewise linear, $\Delta\bar{\Phi} = 0$ inside each triangle Ω_e and, therefore, $\left(\Delta\bar{\Phi}, \nabla_v\bar{\Psi}\right) = 0$. Let us omit the overbar for convenience. Then the equation is reduced to the form

$$K(\nabla\Phi, \nabla\Psi) + \delta\left(\nabla_v\Phi, \nabla_v\Psi\right) + \left(\nabla_v\Phi, \Psi\right) = \left(f, \Psi + \delta\nabla_v\Psi\right).$$

The difference from the standard Galerkin method consists in the presence of the terms $\delta\left(\nabla_v\Phi, \nabla_v\Psi\right)$ and $\delta\left(f, \nabla_v\Psi\right)$. Integrating the term $\delta\left(\nabla_v\Phi, \nabla_v\Psi\right)$ formally by parts, we obtain $-\delta\left(\nabla_{vv}\Phi, \Psi\right)$, $\nabla_{vv}\Phi$ denotes the second derivative of Φ in the direction v. This means that the Petrov — Galerkin method can be interpreted as the addition of artificial viscosity of δ in the direction of the flow v. The term $\delta\left(\nabla_v\Phi, \nabla_v\Psi\right)$ is also numerically discretized in a similar way, as the diffusion term in the standard Galerkin method. Further calculations are performed in the same way as in the standard Galerkin method.

And, finally, the parameter δ is given as $\delta = 0\left(\dfrac{h}{v}\right)$, where h is a typical grid cell size. Numerical experiments have shown that the values $\delta = c\dfrac{h}{v}$, where $0.2 \leq c \leq 1.5$, give quite satisfactory results.

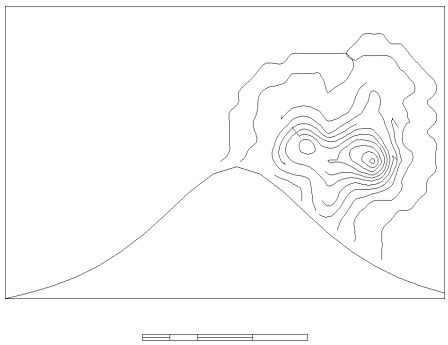

Fig. 1.

Thus, let us point out the main difference between the Petrov — Galerkin method and the standard Galerkin method. The Petrov — Galerkin method is based on test functions of the form $\Psi + \delta \nabla_v \Psi$, where Ψ is piecewise linear and continuous. In particular, the test functions are discontinuous due to the discontinuity of the term $\delta \nabla_v \Psi$. This means that the test functions belong to a space that differs from the space of test functions where the discrete solution Φ is sought for. On the other hand, in the standard Galerkin method the spaces of simple and test functions coincide.

Figure 1 shows a typical calculated pattern for the transport of a substance over a bell-shaped hill at a standard atmospheric stratification of 3.5 K/km and a horizontal geostrophic wind of 5 m/s. The necessary meteorological data are obtained from the model described in the next section.

3. Coastal site flow simulation

In this Section, we apply the nonhydrostatic and hydrostatic versions of the above model to simulating the dynamic pressure effects caused by changes in roughness and interaction of the flow with a low terrain. For this purpose, we consider flow over a low hill at a coastal site [5].

The height of the hill is about 3 meters, which is achieved gradually at a distance of about 50 meters. The roughness coefficient is 0.001 cm for water and 1.00 cm for land (grass).

The observations were performed at three 12-m masts having instruments at 1-, 2-, 3-, 5-, 8-, and 12-m levels. The topography of the domain and the location of the three masts are shown in fig. 2. The measurements of the horizontal wind speed were taken on 17 October 1974 and were reported by Peterson et al. [5] and Takle et al. [4].

As reported by Takle et al. [4], notable features of the wind speed profiles are that the low-level flow experiences a decrease in speed due to the increased roughness. At the upper levels, there is an increase in the wind speed caused by the increase in terrain elevation.

Takle et al. [4] have shown that these effects cannot be realistically simulated with a hydrostatic model. They used the procedure of Song et al. [2] for parameterizing nonhydrostatic terrain effects into their hydrostatic model.

Instead of this, in this paper the nonhydrostatic version of the model described in the previous section was used and compared with the hydrostatic version of the same model. The simulation results are shown in figures 3 and 4 for observations performed at mast 2 (located at a distance of about 70 meters from the shore). The initial conditions were a neutral temperature profile and a wind field driven by a 10 m/s wind at the top. Figures 3 and 4 show

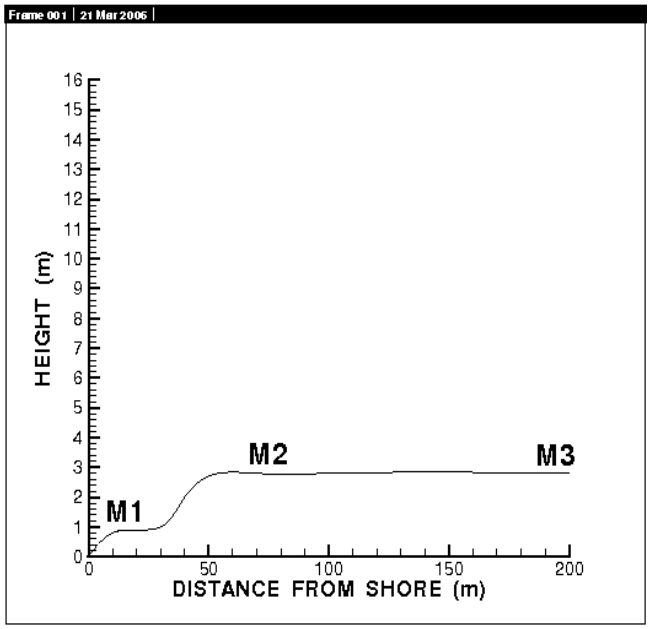

Fig. 2.

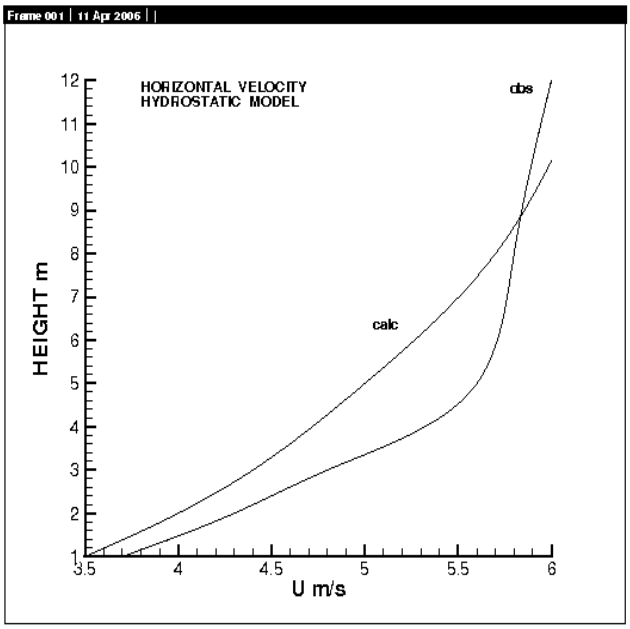

Fig. 3.

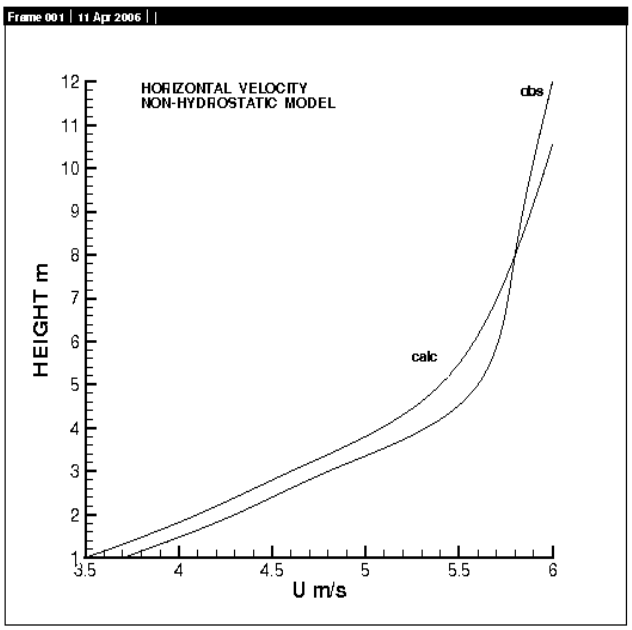

Fig. 4.

horizontal velocity observations versus calculation velocities produced by the hydrostatic and nonhydrostatic versions, respectively. It is evident that the nonhydrostatic version gives much better results in comparison with the hydrostatic version.

It is not an easy task to compare in detail our results with simulations performed in [3] by using the procedure of Song et al. [2], because some important parameters of the calculations may be different. In general, the agreement is good and, therefore, the direct application of the nonhydrostatic model to simulating land-water boundary flows can be considered as a useful

alternative to the procedure proposed in [2] and [3].

Conclusions

We have described an application of hydrostatic and nonhydrostatic versions of a small-scale meteorological model to simulating flows that occur at water-land boundaries. The results obtained above have shown that the nonhydrostatic version of the model has improved significantly the results produced by the hydrostatic version. It has been shown that the nonhydrostatic model can be used to simulate realistically the effects of flows that are subject to dynamic influence of low terrain features and roughness changes at water-land boundaries.

References

[1] Pielke R.A. Mesoscale Meteorological Modeling. Orlando: Acad. Press, Fla, 1984.

[2] Song J.L., Pielke R.A., Segal M. et al. A method to determine nonhydrostatic effects within subdomains in a mesoscale model // J. Atmos. Sci. 1985. Vol. 42. P. 2110–2120.

[3] Takle E.S., Russell R.D. Modeling the atmospheric boundary layer // Comput. Math. Applic. 1988. Vol. 16, N 1/2. P. 57–68.

[4] Yudin M.S. Numerical simulation of orographic waves using an atmospheric model with artificial compressibility // Bull. Nov. Comp. Center, Num. Model. in Atmosph. 1995. Vol. 2.

[5] Peterson E.W., Taylor P.A., Hojistrup J. et al. Riso 1978: Further Investigations into the Effects of Local Terrain Irregularities on Tower-Measure Wind Profiles // Boundary–Layer Meteorology. 1980. Vol. 19. P. 303–313.

[6] Marchuk G.I. Mathematical Modelling in the Problem of the Environment. Amsterdam: North Holland, 1982.

[7] Brooks A., Hughes T. Streamline upwind Petrov-Galerkin formulations for convection dominated flows with particular emphasis on the incompressible Navier — Stokes eguations // Comput. Meth. Appl. Mech. Eng. 1982. Vol. 32. P. 199–259.

Received for publication 9 November 2006